JPMB | Journal of Plant Molecular Breeding
Published by Genetics and Agricultural Biotechnology Institute of Tabarestan
2023 | Volume 11 | Issue 1

Molecular cloning and *in silico* analysis of a GTP cyclohydrolase I gene from grape

Nadia Eslami-Bojnourdi, Raheem Haddad*, Ghasem-Ali Garoosi, Reza Heidari-Japelaghi

Department of Biotechnology Engineering, Faculty of Agricultural and Natural Resources, Imam Khomeini International University, Qazvin, Iran

Original paper

OPEN ACCESS

Edited by

Prof. Ahmad Arzani,
Isfahan University of Technology, Iran

Date

Received 25 February 2023
Accepted: 8 October 2023
Published: 25 January 2024

Correspondence

Dr. Raheem Haddad
r.haddad@eng.ikiu.ac.ir

Citation

Eslami Bojnourdi, N., Haddad, R., & Heidari-Japelaghi, R. (2023). Molecular cloning and *in silico* analysis of a GTP cyclohydrolase I gene from grape.*J. Plant Mol. Breed 11* (1): 1-16. 10.22058/JPMB.2023.1990428.1271.

Abstract: An entire open reading frame (ORF) encoding for a polypeptide of GTP cyclohydrolase I (GTPCH I) was isolated and cloned from Askari cultivar of grape (*Vitis vinifera* L.) berries. The 1,338-nucleotide ORF yields a 445-residue amino acid sequence with a calculated molecular mass of 48.65 kDa and a predicted isoelectric point of 6.43. The *Vvgtpch* I genomic sequence with a length of 4,964 bp contains two exons (169 and 1,169 bp) and an intron (2,676 bp). The *gtpch* I sequence of grape displayed a strong similarity with *gtpch* I sequence found in other plants, including peach (72%), cocoa (72%), strawberry (70%), and poplar (69%). Analysis of mRNA secondary structure revealed that the start codon of *Vvgtpch* I is completely exposed, suggesting a robust binding of the ribosome and efficient translation. Similar to *gtpch*s I from diverse sources, molecular modeling uncovered that the monomer of VvGTPCH I adopts an $\alpha\beta$ structure, which includes 10 α-helices and 8 β-sheets. Moreover, *in silico* analysis of the *Vvgtpch* I gene promoter identified potential *cis*-acting elements responsive to environmental signals. This suggests that the *Vvgtpch* I gene has the capacity to be responsive to various environmental cues, such as heat, heavy metals, light, and plant hormones.

Keywords: folate, *in silico* analysis, regulatory elements, cloning, promoter region

Introduction

GTP cyclohydrolase I (GTPCH I, EC 3.5.4.16) plays a role in the conversion of GTP to dihydroneopterin triphosphate and formic acid. This reaction represents the initial and essential stage in the biosynthesis of tetrahydrofolate (FH_4) in plants and certain microorganisms, as well as tetrahydrobiopterin (BH_4) in mammals (Blau and van Spronsen, 2013) (Figure 1). Folates are part of a wide-ranging family of polyglutamates derived from pteroic acid and its related analogs. They play a vital role as cofactors in the synthesis of purines, pyrimidines, pantothenate, thymidylate, and in the metabolism of various amino acids, such as methionine, serine, and glycine (Blancquaert et al., 2014). Folates are comprised of a p-aminobenzoate (PABA) unit that is fused with a pterin ring derived from GTP, along with a varying number of glutamate moieties. PABA is synthesized from chorismate in the plastid, whereas the pterin unit is produced in the cytosol through the catalytic activity of *gtpch* I (Basset et al., 2004). The last stages of folate synthesis involve the conjugation of PABA and pterin, as well as the incorporation of glutamate moiety. These steps are catalyzed by a series of five enzymes in the mitochondria (Basset et al., 2002).

Insufficient intake of folate in the diet can lead to a decrease in the ability to produce DNA and sustain normal cell division rates. As a direct consequence, folate deficiency primarily leads to the development of megaloblastic anemia, characterized by a decrease in the production of cells in the bone marrow due to impaired biosynthesis. Insufficient levels of this nutrient have been linked to the occurrence of neural tube defects in infants, including conditions like spina bifida and anencephaly (Shlobin et al., 2020). Additionally, it has been found to elevate the risk of vascular disease, certain types of cancer, and cerebral folate deficiency syndromes during childhood (Shlobin et al., 2020; Rossignol and Frye, 2021; Gofir et al., 2022). Research studies with controlled conditions have demonstrated that the addition of folic acid to grain products has resulted in a notable decrease in the occurrence of neural tube defects, specific childhood cancers, and stroke (Gorelova et al., 2017; Strobbe and Van Der Straeten, 2017). Therefore, consuming folates in their natural form, which can be found in abundant quantities in various plant-based foods such as grapes, is an effective strategy to prevent folate deficiency.

Increasing folate biosynthesis through metabolic engineering was the first proposed strategy to biofortify plants (Agyenim-Boateng et al., 2023). The sole introduction of *gtpch* I has led to an enhancement of folate levels in lettuce, rice, Mexican common bean, maize, and wheat (Nunes et al., 2009; Dong et al., 2014; Ramírez Rivera et al., 2016; Liang et al., 2019). The overexpression of *gtpch* I increased folate levels in rice by 3.3 to 6.1-fold (Dong et al., 2014) and enhanced lettuce folates by 2.1 to 8.5-fold (Nunes et al., 2009). It has been reported that folates in stored rice grains are unstable, which reduces the potential benefits of folate biofortification. Blancquaert et al. (2015) obtained folate concentrations that are up to 150-fold higher than those of wild-type rice by complexing folate to folate-binding proteins to improve folate stability, thereby enabling long-term storage of biofortified high-folate rice grains. The Mexican common bean (*Phaseolus vulgaris* L.) was metabolically engineered by overexpressing *gtpch* I, which increased folate and pteridine levels in the seeds by 3-fold and 150-fold, respectively (Ramírez Rivera et al., 2016). Liang et al. (2019) cloned and co-overexpressed two key soybean folate biosynthesis genes, *Gm8gGCHI* (GTP cyclohydrolase I) and *GmADCS* (aminodeoxychorismate synthase) in maize and wheat. A 4.2-fold and 2.3-fold increase in folate levels were observed in transgenic maize and wheat grains, respectively. Folates serve as suppliers of methyl groups, playing a crucial role in methylation reactions. These reactions are not only vital for controlling gene expression but also play a significant role in the synthesis of proteins, lipids, chlorophyll, and lignin in the plant kingdom (Gorelova et al., 2017; Strobbe and Van Der Straeten, 2017). To the best of our knowledge, there has been limited research conducted on the characterization of the *gtpch* gene in grapes (*Vvgtpch*). Our objective was to isolate and characterize a *Vvgtpch* I gene from Askari cultivar of grape (*Vitis vinifera*) berries. Through *in silico* analysis, we found that the promoter region of *Vvgtpch* I gene is rich in potential regulatory elements, suggesting its potential response to various environmental signals.

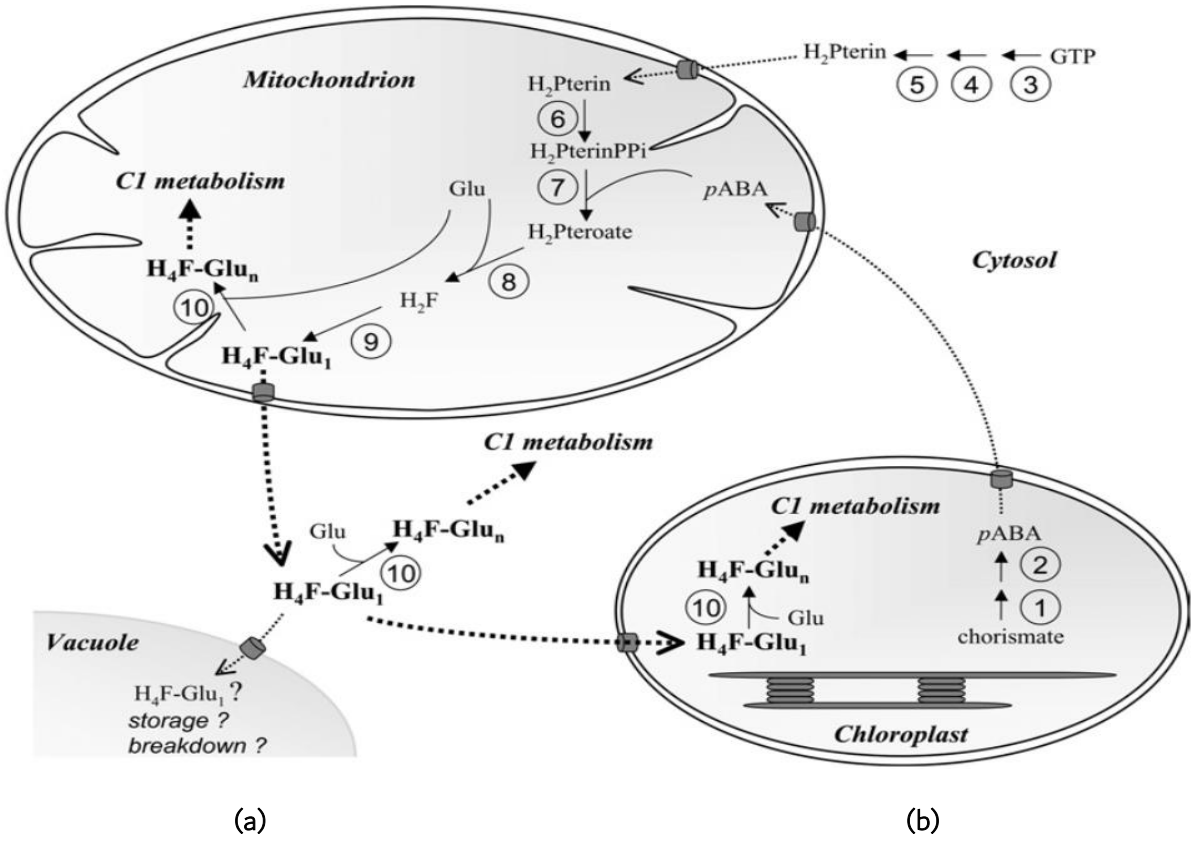

Figure 1. The FH_4 biosynthetic pathway in plants. The enzymes involved in the synthesis of FH_4-Glunare as follows: 1, Aminodeoxychorismate synthase; 2, Aminodeoxychorismate lyase; 3, GTP cyclohydrolase I; 4, Nudixhydrolase; 5, Dihydroneopterin aldolase; 6, Hydroxymethyl dihydropterin pyrophosphokinase (HPPK); 7, Dihydropteroate synthase (DHPS); 8, dihydrofolate synthetase (DHFS); 9, dihydrofolate reductase (DHFR); and 10, folylpolyglutamate synthetase (FPGS) (Sahr et al., 2005).

Materials and Methods

Plant materials and extraction of total RNA

Fresh berries from the cultivar Askari were obtained from grape plants cultivated in the grape collection of the Grape Research Station, Takistan-Qazvin, Iran, in the 2018. Upon collection, all samples were promptly frozen in liquid nitrogen and subsequently stored at -80 ºC. At the veraison stage, seeds were carefully removed from the berries by gently breaking them open in liquid nitrogen. Total RNA was also isolated from fresh grape berries using Cetyltrimethylamonium bromide (CTAB) procedure suggested by Japelaghi et al. (2011).

RT-PCR and molecular cloning

For first strand cDNA synthesis, 5 µg of total RNA treated with *DNase* I (Thermo Fisher Scientific) was used as a template using Oligo $(dT)_{18}$ primer (1 µg/µl, Qiagen) for 5 min at 70 ºC. The reaction mixture was incubated with RevertAid™ M-MuLV Reverse Transcriptase (200 u/µl, Thermo Fisher Scientific) for 60 min at 42 ºC. The mixture was brought to a halt by subjecting it to heat at 70 ºC for 10 min. The degenerate primers (Dgtpch IF: 5′-ATGGGNGCNCTNGAYGARGGN-3′; Dgtpch IR: 5′- NGANGTNGCNGTRTTNGGDAT-3′) used in this study were designed based on the available expressed sequence tags (ESTs) from *Prunus persica*, *Theobroma cacao*, and *Populus trichocarpa*, identified with the BLASTn program (http://www.ncbi.nlm.nih.gov) for the amplification of the *Vvgtpch* I gene by the reverse transcription-PCR (RT-PCR). The RT-PCR reaction was carried out in a thermal cycler (Techene, UK) programmed for 35 cycles; conditions for each cycle being denaturation at 94 ºC for 30 s, annealing at 45 ºC for

min, and extension at 72 ºC for 1 min. The final extension was performed at 72 ºC for 5 min. The PCR products were purified using the AccuPrep Gel Purification kit (Bioneer, South Korea), following the manufacturer's instructions. Subsequently, the purified products were subcloned into the pTG19-T vector (Vivantis, Malaysia) as per the manufacturer's guidelines. The dideoxynucleotide sequencing (Bioneer, South Korea) was used to determine the nucleotide sequence of the inserts in both directions.

Sequence analysis

The estimated properties of the deduced amino acid sequence were obtained using ProtParam program (http://www.expasy.ch/tools/protparam.html), while its subcellular localization prediction was conducted by combining three different programs, TargetP (http://www.cbs.dtu.dk/services/TargetP/), iPSORT (http://ipsort.hgc.jp/) and YLOC (http://www-bs.informatik.uni-tuebingen.de/Services/YLoc/). The prediction of functional domains was carried out using the MotifScan program (https://myhits.isb-sib.ch/cgi-bin/motif_scan), while the identification of potential sites for post-translation modifications (PTM) was performed using the ScanProsite program (https://prosite.expasy.org/scanprosite/). The mRNA sequence was submitted to the RNAfold WebServer (Vienna RNAWebsuite) (http://rna.tbi.univie.ac.at/cgi-bin/RNAWebSuite/RNAfold.cgi) to predict its secondary structure and calculated the minimum free energy (MFE) based on base-pair probabilities. PSIpred (http://bioinf.cs.ucl.ac.uk/psipred/) was used to predict the secondary structure of VvGTPCH I, while the I-TASSER program (http://zhang.bioinformatics.ku.edu/I-TASSER) was employed to predict its three-dimensional (3D) structure.

Analysis of promoter region

The promoter region of the grape *Vvgtpch* I gene was sourced from the Phytozome website (http://www.phytozome.net) and analyzed using PlantCare software (http://bioinformatics.psb.ugent.be/webtools/plantcare/html/) to identify regulatory elements associated with various types of plant stress responses.

Phylogenetic analysis

Using the *Vvgtpch* I sequence as a query, protein sequences from different organisms or microorganisms were selected by retrieving data from the GenBank via the BLASTp algorithm at the National Center for Biotechnology Information (NCBI). Sequences were aligned using the ClustalX software and a phylogenetic tree was also constructed with MEGA 4.0.2 software via Neighbor Joining method (Tamura et al., 2007).

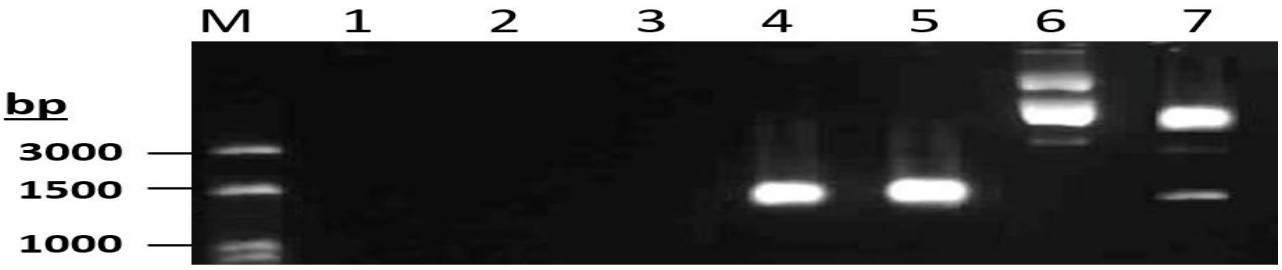

Figure 2. Confirmation of the recombinant pTG19-gtpch I plasmid by PCR, enzyme digestion and 1.2% agarose gel electrophoresis. M) 100 bp DNA ladder, 1) PCR negative control without primers, 2) PCR negative control without template, 3) PCR negative control with bacterial DNA as a template, 4) the *Vvgtpch* I gene amplified in PCR via screening of recombinant clones, 5) the *Vvgtpch* I gene amplified in PCR containing the recombinant pTG19-gtpch I plasmid as a template, 6) The recombinant pTG19-gtpch I plasmid, 7) The recombinant pTG19-gtpch I plasmid digested with *BamH* I.

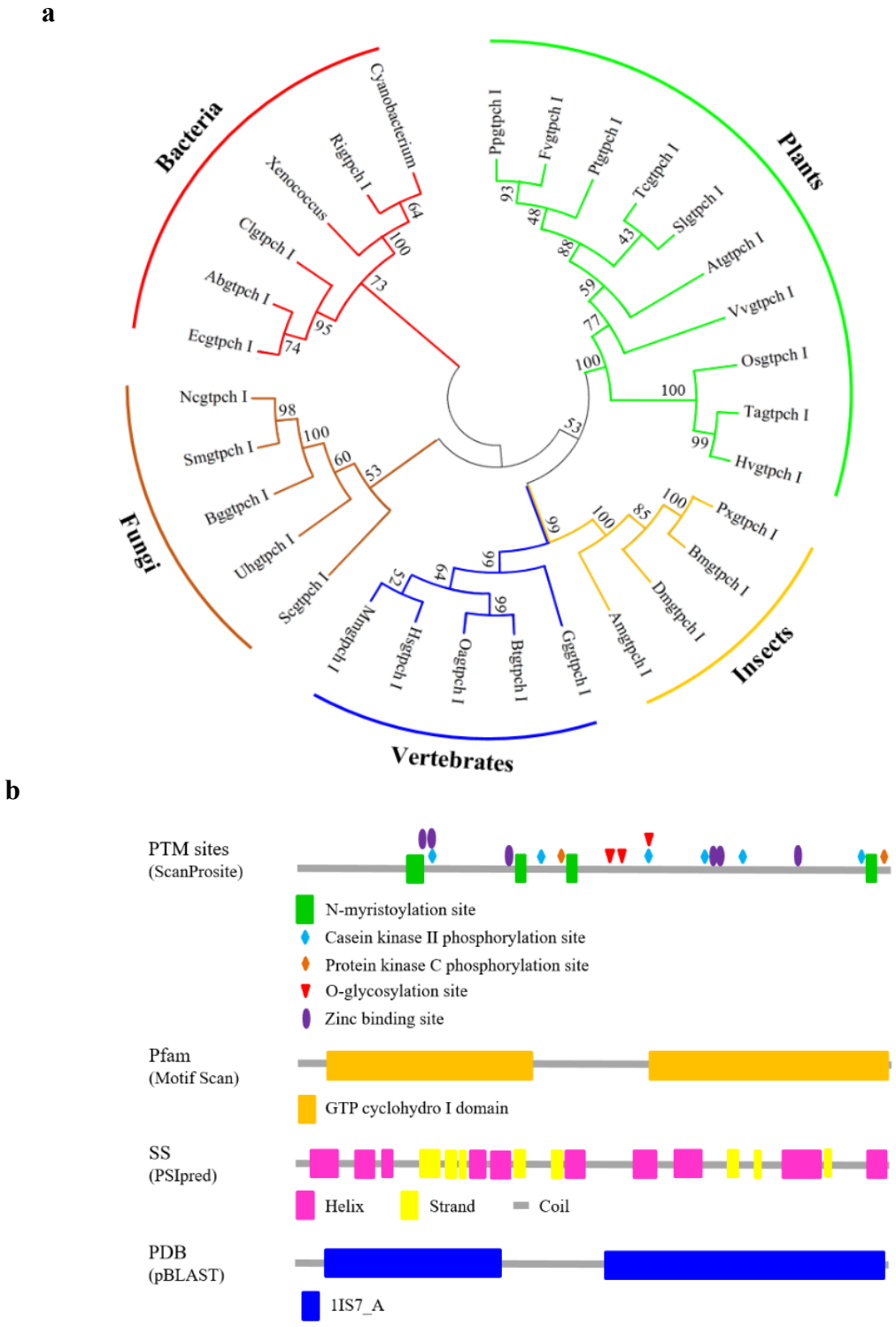

Figure 3. Phylogenetic analysis and structural characterization of *Vvgtpch* I. (**a**) Phylogenetic tree of *Vvgtpch* I and *gtpch*s I from different sources using MEGA 4.0.2 software. (**b**) Multiple sequence alignments of *Vvgtpch* I and *gtpch* I sequences from plants. The protein sequence deduced from the *Vvgtpch* I gene was aligned with its homologs from different plants using ClustalX. The *Vvgtpch* I signature sequences are indicated in black boxes. (Continue in next page)

c

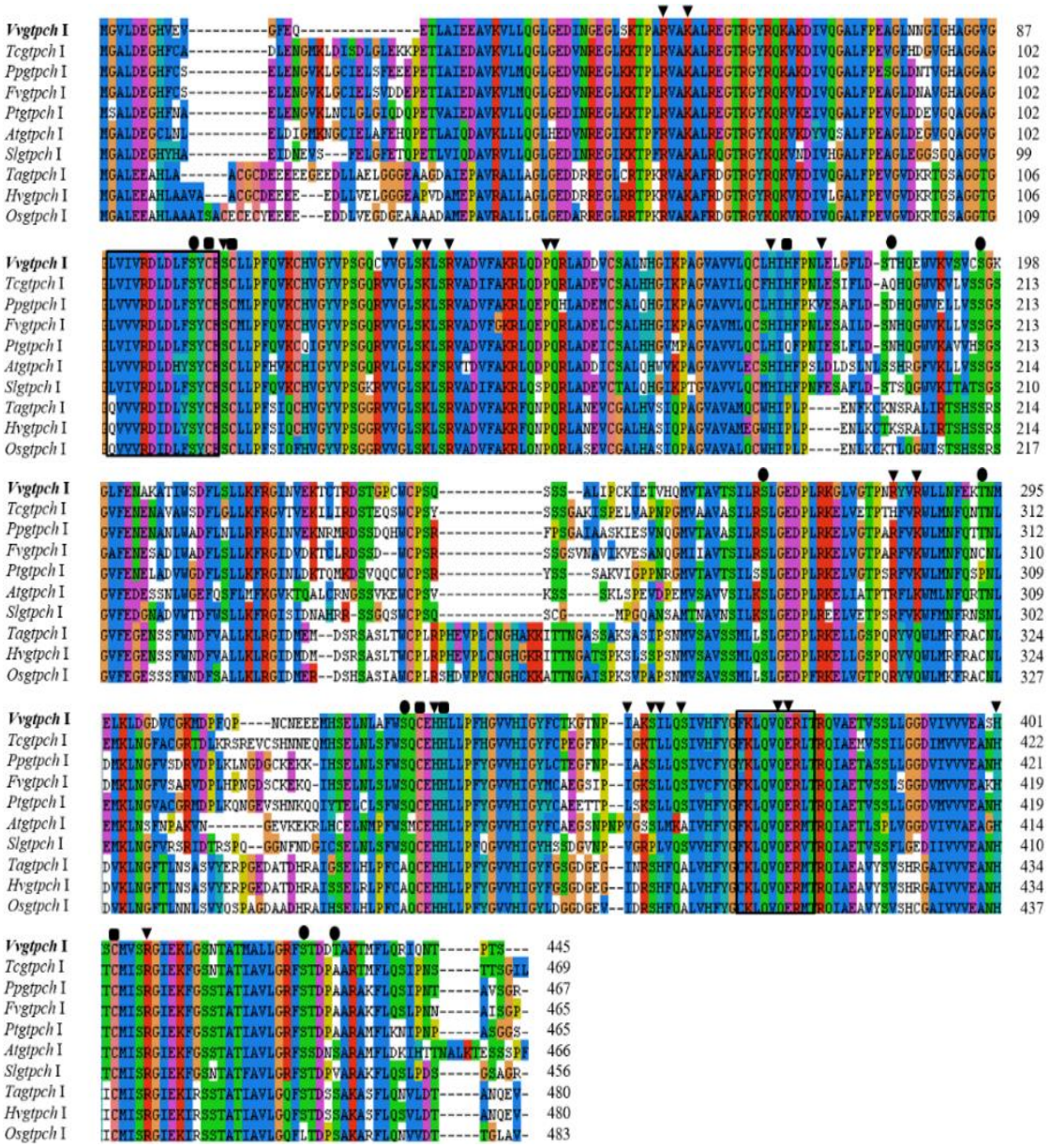

The conserved active site residues, residues involvement in zinc binding, and the possible phosphorylation sites for protein kinase C and casein kinase II are shown by black triangles, squares, and circulars, respectively. The NCBI and EMBL accession numbers for the sequences described and mentioned in this study are as follows: *Apis mellifera* (*Amgtpch* I, XP_624456.2), *A. thaliana* (*Atgtpch* I, NP_187383), *Arcobacter butzleri* (*Abgtpch* I, YP_008331555), *Blumeria graminis* (*Bggtpch* I, EPQ61888), *Bombyx mori* (*Bmgtpch* I, NP_001166803), *Bos Taurus* (*Btgtpch* I, XP_002690995), *Cellulophaga lytica* (*Clgtpch* I, YP_004263693), *Chlamydomonas reinhardtii* (*Crgtpch* I, NW_001843677), *Cyanobacterium* spp. (WP_017322947), *E. coli* (*Ecgtpch* I, EU747840), *Fragaria vesca* (*Fvgtpch* I, XP_004290171), *G. gallus* (*Gggtpch* I, NP_990554), *Homo sapiens* (*Hsgtpch* I, AAN17459), *Hordeum vulgare* (*Hvgtpch* I, BAJ95470), *Neurospora crassa* (*Ncgtpch* I, XP_958695), *O. sativa* (*Osgtpch* I, EAZ32303), *Ovis aries* (*Oagtpch* I, XP_004011081), *Papilio xuthus* (*Pxgtpch* I, BAE66650), *P. trichocarpa* (*Ptgtpch* I, XP_002320619), *P. persica* (*Ppgtpch* I, EMJ02205), *Richelia intracellularis* (*Rigtpch* I, WP_008234507), *Saccharomyces cerevisiae* (*Scgtpch* I, CAA87397), *Solanum lycopersicum* (*Slgtpch* I, NP_001234141), *Sordaria macrospora* (*Smgtpch* I, XP_003345165), *Triticum aestivum* (*Tagtpch* I, ABM54074), *T. cacao* (*Tcgtpch* I, EOX93821), *Ustilago hordei* (*Uhgtpch* I, CCF48468), *Xenococcus* sp. (WP_006509939). (**c**) The potential sites for PTMs and the functional domains were predicted using ScanProsite and MotifScan. The secondary structure of *Vvgtpch* I was predicted by PSIpred program. The three-dimensional structure of *gtpch* I was retrieved from the PDB through the BLASTp algorithm at NCBI using the amino acid sequence of *Vvgtpch* I a query.

Results

Cloning and sequence analysis of Vvgtpch I gene

Using the degenerate primers, the *Vvgtpch* I gene was isolated and cloned into pTG19-T plasmid vector to generate the recombinant pTG19-gtpch I plasmid (Figure 2). The open reading frame (ORF) of *Vvgtpch* I (submitted at NCBI GenBank under accession number KF891965) was 1,338 nucleotides long and coding for a polypeptide of 445 amino acid residues. The calculated molecular mass and the predicated isoelectric point of the deduced polypeptide sequence are 48.65 kDa and 6.43, respectively. Using the ProtParam program, the Aliphatic, the Hydropathicity, and the Instability indexes were evaluated about 93.69, -0.016, and 38.32, repectively. The lack of an N-terminal extension indicates that the *Vvgtpch* I protein is likely localized in the cytosol. This proposal is further supported by the analysis conducted using three programs: TargetP, iPSORT, and YLOC.

Phylogenetic analysis

The *Vvgtpch* I and *gtpch* I sequences from various organisms or microorganisms were utilized to construct a phylogenetic tree (Figure 3a). The tree exhibits two prominent clusters. One cluster contains plants and the other includes non-plants. The first cluster consists of bacteria, fungi, insects, and vertebrates, while the second cluster has two main branches, including monocotyledons and dicotyledons. The grape *gtpch* I displays a strict identity with *gtpch* I sequences from other plants, such as peach (*P. persica*; *Ppgtpch* I, 72%), Cocoa (*T. cacao*; *Tcgtpch* I, 72%), Poplar. (*P. tricocarpa*; *Ptgtpch* I, 69%), and strawberry (*F. vesca*; *Fvgtpch* I, 70%) (Figure 3b). In contrast, the grape *gtpch* I shares lower degree of identity to *gtpch* I from human, *S. cerevisiae*, and *Cyanobacterium* with 40, 44, and 45%, respectively. The position of conserved amino acids in active site and other the conserved regions between *Vvgtpch* I and *gtpch*s I from other plants have also been represented in Figure 3b. The prediction of potential sites for PTM and the functional domains were also carried out using ScanProsite and MotifScan, respectively (Figure 3c). Analysis of secondary structure by PSIpred program revealed that the *Vvgtpch* I contains of ten α-helixes and eight β-sheets. By the amino acid sequence of *Vvgtpch* I as a query, the 3D structure of the *gtpch* I from *Rattus norvegicus* (PDB ID code 1IS7_A) with the highest score (E-value = 9e-23) was retrieved from the Protein DataBase (PDB) through the BLASTp algorithm at the NCBI (Figure 3c).

Prediction of mRNA secondary structure

The RNA secondary structure was analyzed to assess the mRNA stability of *Vvgtpch* I gene and determine situation of the start codon using RNAfold WebServer (Figure 4).

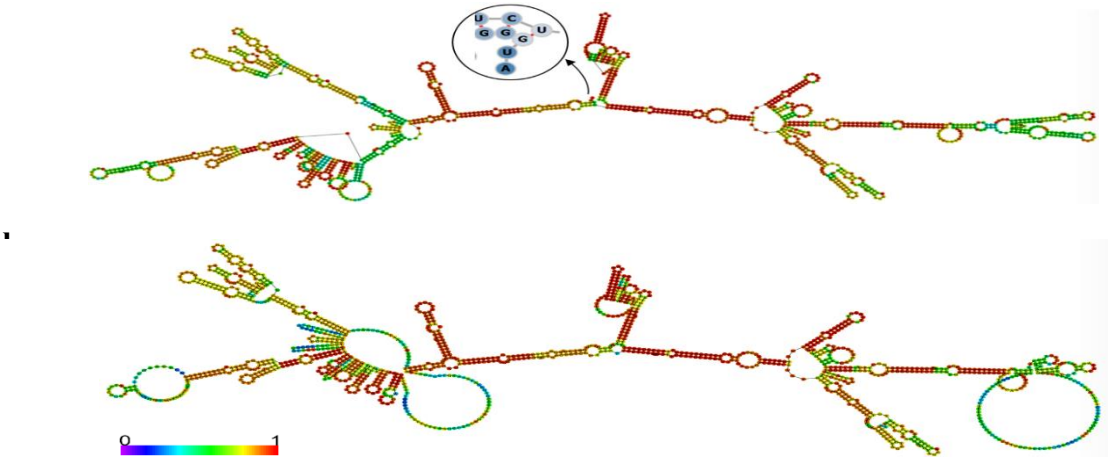

Figure 4. Prediction of mRNA secondary structure of *Vvgtpch* I gene based on the MFE. (**a**) The optimal secondary structure and (**b**) the centroid secondary structure.

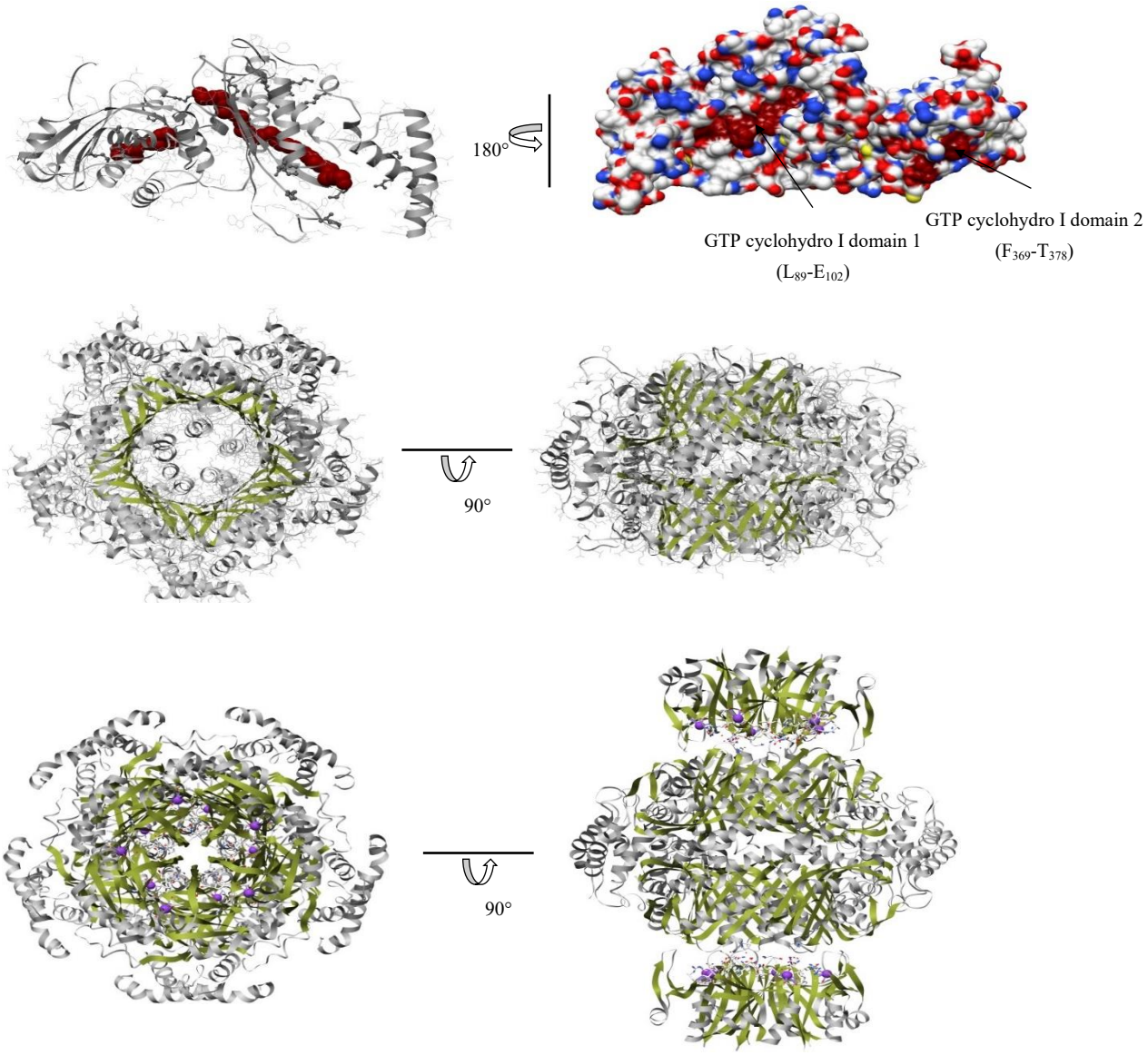

Figure 5. Prediction of three-dimensional model of *Vvgtpch* I and d_5-symmetric homodecamer model of for *gtpch* I. (**a**) Ribbon representation of the monomer structure of *Vvgtpch* I. The signature sequences and the conserved active site residues are indicated by spheres and ball and sticks, respectively. (**b**) View along the molecular 5-fold symmetry axis. The core of the active enzyme complex is formed by a 20-stranded antiparallel β-barrel surrounding five α-helices. (**c**) Complex of GTP cyclohydrolase I/GFRP, viewed along a molecular *c2* axis. The phenylalanine residues are indicated as sphere models.

The mRNA secondary structures emerged to be different in bi-dimensional models and displayed various predicted levels of the MFE. The MFE of the optimal secondary structure and the centroid secondary structure for *Vvgtpch* I mRNA were -405.50, and -344.95 kcal mol^{-1}, respectively. In addition, the start codon was fully exposed in the optimal secondary structure.

Molecular modeling analysis

A predicted 3D structure was determined for *Vvgtpch* I by applying I-TASSER simulation. Similar to all *gtpch*s I from different sources, the monomer of *Vvgtpch* I folds into a αβ structure with 10 α-helices and 8 β-sheets (Figure 5a). In eubacteria and animals, the GTP cyclohydrolases I are structurally

similar and they oligomerize to a toroid-shaped, d_5-symmetric homodecamer (Figure 5b). Figure 5c represents one homodecameric GTP cyclohydrolase I molecule in interaction with two GFRP molecules.

Regulatory elements in the promoter region of Vvgtpch I gene

In order to understand how oxidative stresses regulate the grape *gtpch* I gene, we retrieved its promoter region from the Phytozome website and used the PlantCare software to identify relevant *cis*-acting elements. Analyzing the grape *gtpch* I promoter region revealed the presence of several potential *cis*-acting elements that are known to respond to environmental signals (Figure 6). There are three heat stress responsive elements (HSE) in +223, +631, and -839. A putative basic motif (GGTCCAT) involved in auxin responsiveness was located at position +1045. A sequence similar to the conserved core sequence of metal responsive element (MRE) (TGCAGAC) is found that locates at position +1474. A potential TCA-element (-117) that is believed to be associated with the response to SA (Salicylic Acid) was also discovered. Lastly, in the promoter region of grape *gtpch* I, TC-rich repeats were identified at position +480, implying their potential involvement in stress response. The sequence also includes a proposed TATA box at +1460 relative to the transcriptional start site and a potential CAAT box at +1297. Table 1 show cases additional *cis*-acting elements in the *Vvgtpch* I promoter region, which are responsive to environmental signals.

Figure 6. The nucleotide sequence of promoter region of *Vvgtpch* I gene. The potential cis-acting regulatory elements identified using PlantCare software are shown by color boxes. The putative TATA box at +1460 and the putative CAAT box at +1297 are also underlined.

Table 1. The potential cis-acting regulatory elements identified in the promoter region of *Vvgtpch* I gene using PlantCare software.

Cis-acting elements	Function	Sequence	Numbers	Positions
ARE	Anaerobic induction	TGGTTT	1	-1286
AuxRR-Core	Auxin	GGTCCAT	1	+1045
Box 4	Light	ATTAAT	3	+542, +721, +1064
Box I	Light	TTTCAAA	1	-182
Box II	Light	GTGAGGTAATAT	1	-352
GATA-motif	Light	AAGGATAAGG	1	-693
HSE	Heat stress	AAAAAATTTC	3	+223, +631, -839
MNF1	Light	GTGCCC(A/T)	1	+149
MRE	Heavy metals	TGCAGAC	1	+1474
SP1	Light	CC(G/A)CCC	1	+1395
TC-rich repeats	Defense and stress	ATTTTCTCCA	1	+480
TCA-element	Salicylic acid	CAGAAAAGGA	1	-117

Table 2. Characteristics of nucleotide and amino acid sequences of *Vvgtpch* I and *gtpchs* I from different sources.

Organism	Gene	RefSeq accession no.	Chromosomal position	Strand	Length (bp)				Molecular weight (Da)	Exon: Intron no.
					Gene	mRNA	ORF	Protein (aa)		
S. cerevisiae	*Scgtpch* I	NC_001139	VII	-	1,143	1,143	732	243	27,769	1:0
C. reinhardtii	*Crgtpch* I	NW_001843677	Unknown	+	2,428	630	630	209	22,928	4:3
D. melanogaster	*Dmgtpch* I	NT_033778	57C7-57C8	-	7,294	5,596	975	324	35,541	5:4
H. sapiens	*Hsgtpch* I	NC_000014	14q22.2	-	60,822	2,928	753	250	27,903	6:5
G. gallus	*Gggtpch* I	NC_006092	5	+	16,809	894	711	236	26,115	6:5
M. musculus	*Mmgtpch* I	NC_000080	14C1	-	35,519	2,775	726	241	27,014	6:5
A. thaliana	*Atgtpch* I	NC_003074	3	+	3,367	2,725	1,401	466	51,380	2:1
S. lycopersicum	*Slgtpch* I	NC_015443	6	-	3,273	1,985	1,371	456	49,951	2:1
P. trichocarpa	*Ptgtpch* I	XP_002320619	2	+	3,092	2,274	1,398	465	50,923	2:1
T. cacao	*Tcgtpch* I	CM001879	1	-	2,895	2,106	1,410	469	51,503	2:1
V. vinifera	*Vvgtpch* I	XM_002269229	1	+	4,964	2,288	1,338	445	48,651	2:1

Position of introns in Vvgtpch I and other gtpchs I

The genomic sequence of *Vvgtpch* I spans a length of 4,964 bp. Within this sequence, there are two exons, measuring 169 and 1,169 nucleotides in length, respectively. Additionally, there is an intron present, spanning a length of 2,676 bp. The exon-intron junctions follow the GT-AG rule, similar to how it occurs in higher plants. Additionally, in line with plant genes, the intron in this grape gene contains a relatively higher AT content when compared to the coding regions (Gallie, 1993). The characteristics of nucleotide and amino acid sequences of *gtpch* I genes from different sources have been demonstrated in Table 2. The plant *gtpch* I genes contain a single intron with the diverse size at the conserved position. The size of *Arabidopsis gtpch* I intron is far shorter than that of cacao (789 bp), populus (818 bp), tomato (1,288 bp), and grape (2,676 bp) (Figure 7a). Similar to other plant *gtpch* I genes, the *Vvgtpch* I contains an intron at the same position (50Gly) and the splicing site is between 1–2 nucleotides [1 (g/gt)] (Figure 7b). In plant *gtpch* I genes, the Gly residues place at different positions, nevertheless, their splicing sites are similar with each other. The size and position of introns were also investigated in yeast, *chlamydomonas*, fruit fly, and vertebrates *gtpch* I genes. In yeast, the *Scgtpch* I do not harbor any introns, whereas the *gtpch* I genes from *chlamydomonas*, fruit flies, and humans contain three, four, and five introns, respectively (Figure 7a).

a

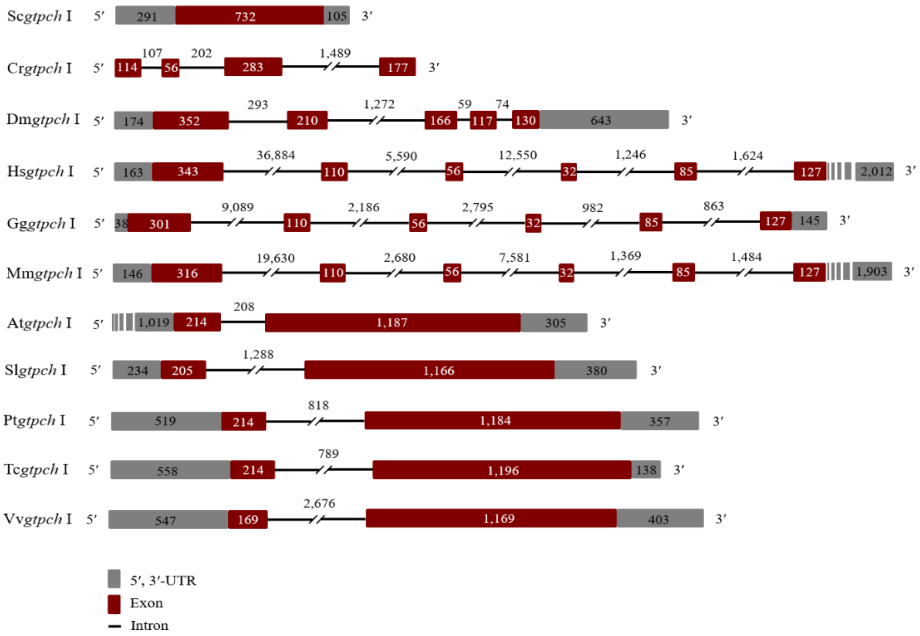

b

```
                                                    10        20        30
Crgtpch I   ----------------------MAPCRDKDKVARMEQAVRVLIHGLGEDLEREGLRDTPKR  39
Dmgtpch I   PGHEKCTFHHDLELDH------KPPTREALLPDMARSYRLLLGGLGENPDRQGLIKTPER 170
Ggtpch I    SGGSGDGWR--GERPR------SEEDNELSLPSLAAAYTTILRALGEDPERQGLLKTPWR  83
Hsgtpch I   SAQPADGWK--GERPR------SEEDNELNLPNLAAAYSSILSSLGENPQRQGLLKTPWR  97
Mmgtpch I   GAQPADAWK--AGRHR------SEEENQVNLPKLAAAYSSILLSLGEDPQRQGLLKTPWR  88
Atgtpch I   GALDEGCLNLELDIGMKNGCIELAFEHQPETLAIQDAVKLLLQGLHEDVNREGIKKTPFR  61
Slgtpch I   GALDEGHYHAEIDNEVSF---ELGFETQPETLVIQDAVRVLLQGLGEDINREGIKKTPFR  58
Vvgtpch I   GVLDEGHVEVG----------------FEQETLAIEEAVKVLLQGLGEDINGEGLSKTPAR  46
Tcgtpch I   GALDEGHFCADLENGMKLDISDLGLEKKPETIAIEDAVKVLLQGLGEDVNREGLKKTPLR  61
Ptgtpch I   SALDEGHFNAELENGVKLNCLGLGIQDQPETVAIEDAVKVLLQGLGEDINREGLKKTPLR  61

                    40        50        60        70                  80        90
Crgtpch I   VAKALLDCTQGYHQDTSSTLGTALFHEPIVHD------GDEGVVLVRDIDFASTSEETLL  93
Dmgtpch I   AAKAMLYFTKGYDQSLEDVLNGAVFDED----------HDEMVVVKDIEMFSMCEHHLV 219
Ggtpch I    AATAMQFFTKGYQETIADVLNDAIFDED----------HDEMVIVKNIDMFSLCEHHLV 132
Hsgtpch I   AASAMQFFTKGYQETISDVLNDAIFDED----------HDEMVIVKDIDMFSMCEHHLV 146
Mmgtpch I   AATAMQYFTKGYQETISDVLNDAIFDED----------HDEMVIVKDIDMFSMCEHHLV 137
Atgtpch I   VAKALREGTRGYKQKVKDYVQSALFPEAGLDEGVGQAGGVGGLVVVRDLDHYSYCESCLL 121
Slgtpch I   VAKALRQGTRGYKQKVNDIVHGALFPEAGLEGGSGQAGGVGGLVIVRDLDLFSYCESCLL 118
Vvgtpch I   VAKALREGTRGYRQKAKDIVQGALFPEAGLNNGIGHAGGVGGLVIVRDLDLFSYCESCLL 106
Tcgtpch I   VAKALREGTRGYKQKVKDIVQGALFPEVGFHDGVGHAGGAGGLVIVRDLDLFSYCESCLL 121
Ptgtpch I   VAKALREGTKGYKQRVKEIVQGALFPEVGLDDEVGQAGGAGGLVIVRDLDLFSYCESCLL 121

                   100       110       120       130       140       150
Crgtpch I   PFHGRCHVAYRPKNGVVLGLSKLARLTKQYAKRLQTQERLAAEVAHALQQSLECYGIADA 153
Dmgtpch I   PFYGKVSIGYLPCN-KILGLSKLARIVEIFSRRLQVQERLTKQIAVAVTQAVQPAGVAV- 277
Ggtpch I    PFVGKVHIGYLPNK-QVLGLSKLARIVEIYSRRLQVQERLTKQIAIAITEALQPAGVGV- 190
Hsgtpch I   PFVGKVHIGYLPNK-QVLGLSKLARIVEIYSRRLQVQERLTKQIAVAITEALRPAGVGV- 204
Mmgtpch I   PFVGRVHIGYLPNK-QVLGLSKLARIVEIYSRRLQVQERLTKQIAVAITEALQPAGVGV- 195
Atgtpch I   PFHVKCHIGYVPSGQRVLGLSKFSRVTDVFAKRLQDPQRLADDICSALQHWVKPAGVAV- 180
Slgtpch I   PFQVKCHVGYVPSGKRVVGLSKLSRVADIFAKRLQSPQRLADEVCTALQHGIKPTGVAV- 177
Vvgtpch I   PFQVKCHVGYVPSGQCVVGLSKLSRVADVFAKRLQDPQRLADDVCSALNHGIKPAGVAV- 165
Tcgtpch I   PFQVKCHVGYVPSGQRVVGLSKLSRVADIFAKRLQDPQRLADEVCSALHHGIKPAGVAV- 180
Ptgtpch I   PFQVKCQIGYVPSGQRVVGLSKLSRVADVFAKRLQDPQRLADEICSALHHGVMPAGVAV- 180

                   160       170       180                           190
Crgtpch I   GCAGGVMVVCDAAHMCMVARGV---ENHSGSTTSF-------------AVRGAFASRPDM 197
Dmgtpch I   ------VVE--GVHMCMVMRGVQKINS-----KTVTSTMLGVFRDDP-KTREEFLNLVNS 323
Ggtpch I    ------VIE--ATHMCMVMRGVQKMNS-----KTATSTMLGVFREDP-KTREEFLTLIRS 236
Hsgtpch I   ------VVE--ATHMCMVMRGVQKMNS-----KTVTSTMLGVFREDP-KTREEFLTLIRS 250
Mmgtpch I   ------VIE--ATHMCMVMRGVQKMNS-----KTVTSTMLGVFREDP-KTREEFLTLIRS 241
Atgtpch I   ------VLECSHIHFPSLDLDSLNLSSHRGFVKLLVSSGSGVFEDESSNLWGEFQSFLMF 234
Slgtpch I   ------VLQCMHIHFPNFESAFLD-STSQGWVKITATSGSGVFEDGNADVWTDFWSLLKF 230
Vvgtpch I   ------VLQCLHIHFPNLELGFLD-STHQEWVKVSVCSGKGLFENAKATIWSDFLSLLKF 218
Tcgtpch I   ------ILQCFHIHFPNLESIFLD-AQHQGWVKVLVSSGSGVFENENAVAWSDFLGLLKF 233
Ptgtpch I   ------VLQCLHIQFPNIESLFLD-SNHQGWVKAVVHSGSGVFENELADVWGDFLSLLKF 233
```

Figure 7. The position and size of introns in the *Vvgtpch* I and *gtpch* I genes from different sources. (**a**) Structure of *Vvgtpch* I gene and genes encoding *gtpch* I from different organisms or micro-organisms. The UTRs, coding regions and non-coding regions are indicated in gray boxes, red boxes and black lines, respectively. (**b**) The position of introns in *Vvgtpch* I and other *gtpch*s I from different organisms or micro-organisms. The deduced amino acid sequences of *gtpch*s I were aligned using ClustalW2 and the position of the introns are represented by an arrow. The *Chlamydomonas Crgtpch* I is revealed for numeration and the starting residue of introns is distinguished by a circular and triangles for plants and other organisms or micro-organisms, respectively. Accession numbers are given in the Materials and methods section.

In *Crgtpch* I, the second intron [57S (2 ag/c)] is according to the second intron [57D (1 g/at)] and first intron [57D (1 g/at)] of *D. melanogaster* and human, respectively. Interestingly, the second, third [118R (2 cg/c)], and fourth [166V (2 gt/c)] introns of *D. melanogaster gtpch* I gene are located at the same positions as the first [57D (1 g/at)], third [118R (2 ag/g)], and fifth [166T (2 ac/a)] introns of *Hsgtpch* I, respectively (Figure 7b).

Discussion

The sequence analysis of *Vvgtpch* I gene indicated that it is a thermostable and hydrophilic protein with long half-life (Claverie and Notredame, 2011). Moreover, the phylogenetic analysis of the *Vvgtpch* I revealed that it is clustered with other plant homologs, and thus represents the *Vvgtpch* I orthologs in grape. It has been reported that the *gtpch* I sequences harbor the conserved amino acid signatures which describe essential residues in the two *gtpch* I catalytic regions (Sigrist et al., 2002). The two *gtpch* I signature sequences identified as the GTP cyclohydro I domains are: signature (1), [DENGQST]-[LIVMPF]-[LIVM]-x(1,2)-[KRNQELD]-[DENKGS]-[LIVM]-x(3)-[STG]-x-C-[EP]-H(2) and signature (2), [SA]-x-[RK]-x-Q-[LIVMT]-Q-E-[RNAK]-[LIM]-[TSNV] and consist of preserved residues that are crucial for both GTP binding and the formation of the GTP binding pocket (Nar et al., 1995).

The *Vvgtpch* I signature sequences identified using of the multiple sequence alignments are signature (1) L_{89}VIVRDLDLFSYCE$_{102}$ and signature (2) F_{369}KLQVQERIT$_{378}$. The grape *gtpch* I protein contains the possible phosphorylation sites by protein kinase C and casein kinase II, which are necessary for the correct enzyme activity and the protein folding (Maier et al., 1995). The grape *gtpch* I, like to other plant *gtpch*s I, has retained the amino acids essential for zinc binding including C_{101}, C_{104}, H_{173}, C_{331}, H_{334}, and C_{403}. In *E. coli*, the replacement of Cys_{110}, Cys_{181}, His_{112} or His_{113} by serine affords catalytically inactive mutant proteins with reduced capacity to bind zinc (Rebelo et al., 2003). Furthermore, it seems likely the grape GTPCH I has misplaced the EF-hand-like motif necessary for calcium interaction. The residues recognized as participants in coordinating Ca^{2+} within the conserved EF-hand-like motif are conserved in animals and *E. coli*, but they are not found in plants (Steinmetz et al., 1998). This suggests that calcium binding is not required for activity, although no data exists on its effects on catalytic action.

In an mRNA molecule, the secondary structure is made through the formation of hydrogen bonds between complementary pairs of nucleotides. The mRNA secondary structure is able to affect gene expression via adjustment of transcription, splicing RNA, transcript degradation, and translation. Thus, study of the mRNA secondary structure is crucial to recognize functional activity of a transcript (Proctor and Meyer, 2013). According to reports, the accessibility of the ribosome binding site and the start codon of the mRNA are crucial factors that significantly impact efficient translation (Morowvat et al., 2014). Furthermore, there have been demonstrations showing a direct dependence between the translation levels and the MFE of the ribosome binding site and the start codon. A reduction of MFE by 1.4 kcal mol^{-1} would decrease the gene expression by 10-fold (de Smit and van Duin, 1990). Furthermore, the manipulation of mRNA secondary structure via codon optimization increased the MFE level and improved translation efficiency (Prabhu et al., 2016). In prediction of mRNA secondary structure, the start codon was fully exposed in the optimal secondary structure, showing an efficient binding of the ribosome and active translation.

The determination of 3D structure of the GTP cyclohydrolase I without recognition of the metal requirement of the enzyme was first reported in *E. coli* (Nar et al., 1995). However, crystallographic study of the human GTP cyclohydrolase I illustrated the existence of crucial zinc ions at the active sites (Auerbach et al., 2000). The structure of d_5-symmetric homodecamer consists of a β-barrel that is formed by 20 strands arranged in an antiparallel manner, surrounding a core consisting of five α-helical segments (Steinmetz et al., 1998) and its molecular symmetry signifies one 5-fold and five 2-fold symmetry axes that are perpendicular to the molecular 5-fold axis (Gräwert et al., 2013). In contrast to eubacteria, the GTP cyclohydrolase of animals contains an extended N-terminal region that plays a critical role in the interaction of this enzyme with the GTP cyclohydrolase feedback regulatory protein (GFRP). The GFRP is a c_5-

symmetric, ring-shaped homopentamer and the entire enzyme/inhibitor complex follows d_5 symmetry (Gräwert et al., 2013). Phenylalanine has been revealed to bind at the enzyme/GFRP junctions with a total of 10 topologically equivalent binding sites (Maita et al., 2004).

It has been exhibited that the grape *gtpch* I promoter region harbors the several potential cis-acting elements responding to environmental signals including HSE, MRE, TCA-element, and TC-rich repeats (Amin et al., 1988; Sakai et al., 1996; Stuart et al., 1985; Goldsbrough et al., 1993; Diaz-de-Leon et al., 1993). It has been reported that a functional HSE consists of at least three basic repeats organized in alternating orientations (Amin et al., 1988). Thus, the HSE motif in the *Vvgtpch* I promoter appears to be functional. In addition, the *Vvgtpch* I gene is probably able to response to heavy metals because MRE plays a role in the induction of metallothionein gene expression in animals in response to heavy metal exposure (Stuart et al., 1985). Moreover, in the promoter region of grape *gtpch* I, a potential TCA-element and TC-rich repeats were identified, implying its potential involvement in response to SA and stress (Goldsbrough et al., 1993). The presence of these potential regulatory elements indicates that the promoter region of grape *gtpch* I has the capability to respond to multiple environmental cues such as heat, heavy metals, light, and plant growth regulators (PGR).

Analysis of size and position of introns in *Vvgtpch* I and other *gtpch*s I suggested that the size of the introns is related to the species (Sahrawy et al., 1996). Also, it confirms that although plant *gtpch* I genes have diverged in their amino acid sequences, they may share a common ancestor with having a single intron at position 50 (Meyer et al., 2002). Furthermore, in contrast to plant *gtpch*s I, the *gtpch* I genes from *chlamydomonas*, fruit flies, and humans contain three, four, and five introns, respectively, indicating a concordant reduction or extension of the various introns of a sequence during evolution (Sahrawy et al., 1996). However, no accommodations observed between the position of these introns and intron position of *Vvgtpch* I or higher plants *gtpch* I genes.

Conclusion

The *Vvgtpch* I gene, also known as grape *gtpch* I, was extracted from the grape berry organ of a specific Iranian cultivar named Askari. By constructing a phylogenetic tree, it was determined that the grape *gtpch* I gene grouped together with similar genes found in other plants, indicating a significant degree of similarity and shared identity with *gtpch* I genes from various plant species. The *in silico* analysis demonstrated that the promoter region of *Vvgtpch* I gene contains a number of potential *cis*-acting elements responding to environmental signals. The presence or absence of a *cis*-acting element in a gene promoter could suggest a specific mode of gene regulation. Collectively, possible strategies to target sensitive transcription factors of *gtpch* I gene or its cofactors are suggested based on the updated view of GTP-dependent gene regulation in grape.

Supplementary Materials

No supplementary material is available for this article.

Author Contributions

Methodology, investigation, N.E.B.; conceptualization, supervision, project administration, R.H.; validation, formal analysis, data curation, G.A.G. and R.H.J.; software, writing—original draft preparation, writing—review and editing, R.H.J. All authors have read and agreed to the published version of the manuscript.

Funding

This research received no external funding.

Acknowledgments

No acknowledgments.

Conflicts of Interest

The authors declare no conflict of interest.

References

Agyenim-Boateng, K.G., Zhang, S., Shohag, M.J.I., Shaibu, A.S., Li, J., Li, B., and Sun, J. (2023). Folate biofortification in soybean: challenges and prospects. *Agronomy* 13(1): 241.

Amin, J., Ananthan, J., and Voellmy, R. (1988). Key features of heat shock regulatory elements. *Mol Cell Biol* 8(9): 3761-3769.

Auerbach, G., Herrmann, A., Bracher, A., Bader, G., Gütlich, M., Fischer, M., Neukamm, M., Garrido-Franco, M., Richardson, J., and Nar, H. (2000). Zinc plays a key role in human and bacterial GTP cyclohydrolase I. *Proc Natl Acad Sci* 97(25): 13567-13572.

Basset, G., Quinlivan, E.P., Ziemak, M.J., Díaz de la Garza, R., Fischer, M., Schiffmann, S., Bacher, A., Gregory III, J.F., and Hanson, A.D. (2002). Folate synthesis in plants: the first step of the pterin branch is mediated by a unique bimodular GTP cyclohydrolase I. *Proc Natl Acad Sci* 99(19): 12489-12494.

Basset, G.J., Quinlivan, E.P., Ravanel, S., Rébeillé, F., Nichols, B.P., Shinozaki, K., Seki, M., Adams-Phillips, L.C., Giovannoni, J.J., and Gregory III, J.F. (2004). Folate synthesis in plants: the p-aminobenzoate branch is initiated by a bifunctional PabA-PabB protein that is targeted to plastids. *Proc Natl Acad Sci* 101(6): 1496-1501.

Blancquaert, D., De Steur, H., Gellynck, X., and Van Der Straeten, D. (2014). Present and future of folate biofortification of crop plants. *J Exp Bot* 65(4): 895-906. doi: 10.1093/jxb/ert483.

Blancquaert, D., Van Daele, J., Strobbe, S., Kiekens, F., Storozhenko, S., De Steur, H., Gellynck, X., Lambert, W., Stove, C., and Van Der Straeten, D. (2015). Improving folate (vitamin B9) stability in biofortified rice through metabolic engineering. *Nat Biotechnol* 33(10): 1076-1078.

Blau, N., and van Spronsen, F.J. (2013). "Disorders of phenylalanine and tetrahydrobiopterin metabolism," in *Physician's guide to the diagnosis, treatment, and follow-up of inherited metabolic diseases*. Springer), 3-21.

Claverie, J.-M., and Notredame, C. (2011). *Bioinformatics for dummies.* John Wiley & Sons.

de Smit, M.H., and van Duin, J. (1990). Secondary structure of the ribosome binding site determines translational efficiency: a quantitative analysis. *Proc Natl Acad Sci* 87(19): 7668-7672.

Dong, W., Cheng, Z.-j., Lei, C.-l., Wang, X.-l., Wang, J.-l., Wang, J., Wu, F.-q., Zhang, X., Guo, X.-p., and Zhai, H.-q. (2014). Overexpression of folate biosynthesis genes in rice (*Oryza sativa* L.) and evaluation of their impact on seed folate content. *Plant Foods Hum Nutr* 69: 379-385.

Gallie, D.R. (1993). Posttranscriptional regulation of gene expression in plants. *Annu Rev Plant Biol* 44(1): 77-105.

Gofir, A., Wibowo, S., Hakimi, M., Putera, D.D., and Satriotomo, I. (2022). Folic acid treatment for patients with vascular cognitive impairment: a systematic review and meta-analysis. *Int J Neuropsychopharmacol* 25(2): 136-143.

Goldsbrough, A.P., Albrecht, H., and Stratford, R. (1993). Salicylic acid‐inducible binding of a tobacco nuclear protein to a 10 bp sequence which is highly conserved amongst stress‐inducible genes. *Plant J* 3(4): 563-571.

Gorelova, V., Ambach, L., Rébeillé, F., Stove, C., and Van Der Straeten, D. (2017). Folates in plants: research advances and progress in crop biofortification. *Front Chem* 5: 21.

Gräwert, T., Fischer, M., and Bacher, A. (2013). Structures and reaction mechanisms of GTP cyclohydrolases. *IUBMB life* 65(4): 310-322.

Japelaghi, R.H., Haddad, R., and Garoosi, G.-A. (2011). Rapid and efficient isolation of high quality nucleic acids from plant tissues rich in polyphenols and polysaccharides. *Mol Biotechnol* 49: 129-137.

Liang, Q., Wang, K., Liu, X., Riaz, B., Jiang, L., Wan, X., Ye, X., and Zhang, C. (2019). Improved folate accumulation in genetically modified maize and wheat. *J Exp Bot* 70(5): 1539-1551.

Maier, J., Witter, K., Gutlich, M., Ziegler, I., Werner, T., and Ninnemann, H. (1995). Homology cloning of GTP-cyclohydrolase-I from various unrelated eukaryotes by reverse-transcription polymerase chain-reaction using a general set of degenerate primers. *Biochem Biophys Res Commun* 212(2): 705-711.

Maita, N., Hatakeyama, K., Okada, K., and Hakoshima, T. (2004). Structural basis of biopterin-induced inhibition of GTP cyclohydrolase I by GFRP, its feedback regulatory protein. *J Biol Chem* 279(49): 51534-51540.

Meyer, Y., Vignols, F., and Reichheld, J.P. (2002). Classification of plant thioredoxins by sequence similarity and intron position. *Meth Enzymol* 347: 394-402.

Morowvat, M.H., Babaeipour, V., Rajabi-Memari, H., Vahidi, H., and Maghsoudi, N. (2014). Overexpression of recombinant human beta interferon (rhINF-β) in periplasmic space of *Escherichia coli*. *Iran J Pharm Res* 13(Suppl): 151.

Nar, H., Huber, R., Auerbach, G., Fischer, M., Hösl, C., Ritz, H., Bracher, A., Meining, W., Eberhardt, S., and Bacher, A. (1995). Active site topology and reaction mechanism of GTP cyclohydrolase I. *Proc Natl Acad Sci* 92(26): 12120-12125.

Nunes, A.C., Kalkmann, D.C., and Aragao, F.J. (2009). Folate biofortification of lettuce by expression of a codon optimized chicken GTP cyclohydrolase I gene. *Transgenic Res* 18(5): 661-667.

Prabhu, A.A., Veeranki, V.D., and Dsilva, S.J. (2016). Improving the production of human interferon gamma (hIFN-γ) in Pichia pastoris cell factory: An approach of cell level. *Process Biochem* 51(6): 709-718.

Proctor, J.R., and Meyer, I.M. (2013). C o F old: an RNA secondary structure prediction method that takes co-transcriptional folding into account. *Nucleic Acids Res* 41(9): e102-e102.

Ramírez Rivera, N.G., García‐Salinas, C., Aragão, F.J., and Díaz de la Garza, R.I. (2016). Metabolic engineering of folate and its precursors in Mexican common bean (*Phaseolus vulgaris* L.). *Plant Biotechnol J* 14(10): 2021-2032.

Rebelo, J., Auerbach, G., Bader, G., Bracher, A., Nar, H., Hösl, C., Schramek, N., Kaiser, J., Bacher, A., and Huber, R. (2003). Biosynthesis of pteridines. Reaction mechanism of GTP cyclohydrolase I. *J Mol Biol* 326(2): 503-516.

Rossignol, D.A., and Frye, R.E. (2021). Cerebral folate deficiency, folate receptor alpha autoantibodies and leucovorin (folinic acid) treatment in autism spectrum disorders: a systematic review and meta-analysis. *J Pers Med* 11(11): 1141.

Sahr, T., Ravanel, S., and Rébeillé, F. (2005). Tetrahydrofolate biosynthesis and distribution in higher plants. *Biochem* 33(4): 758-762.

Sahrawy, M., Hecht, V., Lopez-Jaramillo, J., Chueca, A., Chartier, Y., and Meyer, Y. (1996). Intron position as an evolutionary marker of thioredoxins and thioredoxin domains. *J Mol Evol* 42: 422-431.

Shlobin, N.A., LoPresti, M.A., Du, R.Y., and Lam, S. (2020). Folate fortification and supplementation in prevention of folate-sensitive neural tube defects: a systematic review of policy. *J Neurosurg Pediatr* 27(3): 294-310.

Sigrist, C.J., Cerutti, L., Hulo, N., Gattiker, A., Falquet, L., Pagni, M., Bairoch, A., and Bucher, P. (2002). PROSITE: a documented database using patterns and profiles as motif descriptors. *Brief Bioinformatics* 3(3): 265-274.

Steinmetz, M.O., Plüss, C., Christen, U., Wolpensinger, B., Lustig, A., Werner, E.R., Wachter, H., Engel, A., Aebi, U., and Pfeilschifter, J. (1998). Rat GTP cyclohydrolase I is a homodecameric protein complex containing high-affinity calcium-binding sites. *J Mol Biol* 279(1): 189-199.

Strobbe, S., and Van Der Straeten, D. (2017). Folate biofortification in food crops. *Curr Opin Biotechnol* 44: 202-211.

Stuart, G.W., Searle, P.F., and Palmiter, R.D. (1985). Identification of multiple metal regulatory elements in mouse metallothionein-I promoter by assaying synthetic sequences. *Nature* 317(6040): 828-831.

Tamura, K., Dudley, J., Nei, M., and Kumar, S. (2007). MEGA4: molecular evolutionary genetics analysis (MEGA) software version 4.0. *Mol Biol Evol* 24(8): 1596-1599.

JPMB
Journal of Plant Molecular Breeding
Published by Genetics and Agricultural Biotechnology Institute of Tabarestan
2023 | Volume 11 | Issue 1

مقاله پژوهشی

همسانه‌سازی مولکولی و تجزیه و تحلیل *in silico* ژن *Vvgtpch I* از انگور

نادیا اسلامی بجنوردی، رحیم حداد *، قاسمعلی گروسی*، رضا حیدری--جاپلقی

گروه مهندسی بیوتکنولوژی، دانشکده کشاورزی و منابع طبیعی، دانشگاه بین‌المللی امام خمینی (ره)، قزوین، ایران

چکیده: توالی چارچوب خوانش باز (ORF) رمزگردان پلی‌پپتید GTP سیکلوهیدرولاز I (GTPCH I) از بافت حبه انگور (*Vitis vinifera* L. cv. Askari) جداسازی و همسانه‌سازی شد. توالی ORF به طول ۱۳۳۸ نوکلئوتید رمزگردان یک پلی‌پپتید به طول ۴۴۵ اسیدآمینه است. وزن مولکولی و نقطه ایزوالکتریک توالی پلی‌پپتیدی به ترتیب برابر ۴۸/۶۵ kDa و ۶/۴۳ محاسبه شد. توالی ژن *Vvgtpch* I به طول ۴۹۶۴ نوکلئوتید حاوی دو اگزون (۱۶۹ bp و ۱۱۶۹) و یک اینترون (۲۶۷۶ bp) است. بررسی فیلوژنتیکی نشان داد که ژن *Vvgtpch* I شباهت بالایی با توالی‌های *gtpch* I از سایر گیاهان مانند هلو (۷۲٪)، کاکائو (۷۲٪)، ، توت‌فرنگی (۷۰٪) و صنوبر (۶۹٪) دارد. بررسی ساختار دوم توالی mRNA حاصل از ژن *Vvgtpch* I نشان داد که رمز آغازین ATG به شکل آزادانه در ساختار دوم mRNA قرار گرفته و نشان‌دهنده اتصال و ترجمه کارآمد رونوشت توسط ریبوزوم است. مشابه با تمام *gtpch* Iها از منابع مختلف، بررسی مدل‌سازی مولکولی این ژن نشان داد که ساختار منومر توالی پلی‌پپتیدی VvGTPCH I حاوی ۱۰ مارپیچ α و ۸ صفحه β است. علاوه بر این، تجزیه و تحلیل *in silico* ناحیه راه‌انداز ژن *Vvgtpch* I وجود تعدادی عناصر *Cis-acting* پاسخ‌دهنده به پیام‌های محیطی را اثبات نمود. وجود تعدادی عناصر تنظیمی در ناحیه راه‌انداز نشان می‌دهد که ژن *Vvgtpch* I می‌تواند به انواع مختلفی از پیام‌های بیرونی و درونی از قبیل گرما، فلزات سنگین، نور و هورمون‌های گیاهی پاسخ دهد.

کلمات کلیدی: فولات، تجزیه و تحلیل *in silico*، عناصر تنظیمی، همسانه‌سازی، ناحیه راه‌انداز.

ویراستار علمی
دکتر احمد ارزانی،
دانشگاه صنعتی اصفهان، ایران

تاریخ
دریافت: ۶ اسفند ۱۴۰۱
پذیرش: ۱۶ مهر ۱۴۰۲
چاپ: ۵ بهمن ۱۴۰۲

نویسنده مسئول
دکتر رحیم حداد
r.haddad@eng.ikiu.ac.ir

ارجاع به این مقاله
Eslami Bojnourdi, N., Haddad, R., & Heidari-Japelaghi, R. (2023). Molecular cloning and *in silico* analysis of a GTP cyclohydrolase I gene from grape. *J. Plant Mol. Breed 11* (1): 1-16. 10.22058/JPMB.2023.1990428.1271.